Hybrid method coupling molecular dynamics and Monte Carlo simulations to study the properties of gases in microchannels and nanochannels

S. V. Nedea,* A. J. H. Frijns, and A. A. van Steenhoven
Department of Mechanical Engineering, Eindhoven University of Technology, P.O. Box 513, 5600MB Eindhoven, The Netherlands

A. J. Markvoort and P. A. J. Hilbers
Department of Biomedical Engineering, Eindhoven University of Technology, P.O. Box 513, 5600MB Eindhoven, The Netherlands
(Received 17 November 2004; revised manuscript received 27 April 2005; published 12 July 2005)

We combine molecular dynamics (MD) and Monte Carlo (MC) simulations to study the properties of gas molecules confined between two hard walls of a microchannel or nanochannel. The coupling between MD and MC simulations is introduced by performing MD near the boundaries for accuracy and MC in the bulk because of the low computational cost. We characterize the influence of different densities and molecule sizes on the equilibrium properties of the gas in the microchannel. The effect of the particle size on the simulation results is very small in the case of a dilute gas and increases with the density. The hybrid MD-MC simulation method is validated by comparing the results for density and temperature profiles with those of pure MD and pure MC simulations. These results compare well for pure MD and pure MC, as well as hybrid MD-MC, both in the bulk and near the boundaries, when hard-sphere interactions are used. When Lennard-Jones potentials are used to accurately model the interactions between the gas and wall molecules instead, the results of pure MD simulations differ significantly from the pure MC simulations near the boundaries, but the results of the hybrid method compare well with the pure MD results near the wall, and with the pure MC and pure MD results in the middle of the channel. The hybrid method also very accurately simulates the interface between the MD and MC simulation domains. Comparisons between MD, MC, and hybrid MD-MC computational costs are outlined. The speedup when using 50% of the domain for MD simulations and 50% for MC simulations is very small compared to pure MD simulations times, but this speedup increases drastically for more realistic situations where the region near the wall is small compared to the bulk region.

DOI: 10.1103/PhysRevE.72.016705 PACS number(s): 47.11.+j, 47.45.−n, 44.05.+e, 68.08.−p

I. INTRODUCTION

In the process of miniaturizing electronic components, the trend is that the power consumption increases with a factor of 10 every six years [1]. As a result, heat management becomes more and more important in the process of developing and manufacturing microelectronic components. As the limits of current cooling techniques are reached, new microscale cooling techniques will be required to ensure the optimal performance and lifetime of these components. Since local heat sources appear during operation of these devices, local cooling is wanted. Single- and two-phase forced convective flows in microchannels are promising techniques for the cooling of such electronic components.

Microchannel cooling represents a compact and efficient way of transferring heat from a power source to a gas or a liquid. Macroscopic models for heat transfer are not sufficient to describe this cooling mechanism in microstructures. The validity of the continuum approach has been identified with the validity of the Navier-Stokes equations [2]. For a gas, this requires the Knudsen number $\mathrm{Kn}=\lambda/L$, where λ is the mean free path of the molecules and L the physical length of the system) to be small compared to unity, the limit being $\mathrm{Kn}=0.1$. When the characteristic size of the device decreases or when the flow is more rarefied, such that $\mathrm{Kn}>0.1$, the continuum flow model is no longer valid and must be replaced by another model. The governing equations of the flow model must change from the Navier Stokes equations to the Boltzmann equation [2–4], which involves the molecular velocities instead of the macroscopic quantities. To solve this integro-differential equation for the velocity distribution function using conventional finite element or finite difference methods is difficult since the number of independent variables include both those of physical space and those of the velocity space.

The alternative is to use a molecular model where the volume is filled with a large number of discrete molecules and to apply different particle simulation methods. The particle simulation methods we use are molecular dynamics (MD) [5] and the direct simulation Monte Carlo method (DSMC) [2,6–8]. In MD, the time evolution of a set of interacting molecules is followed exactly. Molecules move and collide according to the forces they exert on each other. In DSMC, movements and collisions of particles occur where the collisions are generated stochastically with scattering rates and postcollision velocity distributions determined from the kinetic theory.

Another reason for using particle simulation methods is that microchannel cooling is most efficient when a phase transition is present in the channel, since through evaporation large amounts of heat can be dissipated. For liquids, a continuum approach can be used up to nano-scale but the phase transition from liquid to vapor cannot be described by a con-

*Electronic address: S.V.Nedea@tue.nl.

tinuum approach. Therefore, the interface has to be specified at a molecular level. The small-scale effects near the walls and at the phase boundaries are best described with a particle simulation method like MD.

MD simulations are able to simulate these effects near the solid wall and near the boundaries of areas of phase transitions accurately. However, because all the pair interactions between all particles have to be calculated, the MD method is too time-consuming for the number of particles needed to simulate a dense gas flow in a microchannel.

However, in the bulk of the channel, the boundary effects are small and therefore the computation can be sped up by using an alternative method like MC, where several molecules can be confined inside one artificial particle. For a dense gas the governing equation of the flow model is an extension of the Boltzmann equation, called the Enskog equation [9–11]. Different MC particle simulation methods have been proposed to solve this equation. The first method described by Garcia [6,7] is an attempt to bring into DSMC [2] the spatial correlations which are absent in an ideal gas. This method encounters problems with boundary conditions when walls are introduced. A particle method for the numerical solution of the Enskog equation has been presented by Montanero and Santos [12] extending the scheme originally proposed by Nanbu [13] for the Boltzmann equation. The method correctly reproduced the transport properties of the Enskog gas, but inherited from the original Nanbu scheme the feature of conserving momentum and energy only in a statistical way and not in a single collision. The particle method proposed by Frezzotti [3] constructed for the Enskog equation in the spirit of the DSMC method exactly conserves momentum and energy. We use this latter method for our MC simulations.

For high-density gas to the limit border with liquid phase, the MC model is not able to describe the small-scale and boundary effects in microchannels and nanochannels well. The liquid flow boundary effects inside microchannels and nanochannels have to be studied using another approach.

The solution is then to use a hybrid approach able to interplay between the simulation of the atomistic processes occuring within a small region of the system and the simulation of slow dynamic processes within the bulk. This requires new methods that can retain the benefit of the atomistic description of matter, where it is really needed, while treating the bulk of the system by much less costly methods.

Several hybrid algorithms of this sort have been proposed in the literature, both for the hybrid MC-continuum approach [14,15], and for the MD-continuum approach [16–18]. As we are interested in the behavior of dense gases in narrow channels, the continuum approach starts to fail [19] and particle-based methods have to be used. Our goal is to couple the MD and MC methods in order to be able to simulate dense gases also in relatively small channels (10–20 times the molecular diameter) efficiently.

In this paper we present a hybrid method to combine the advantages of the MD and MC simulations, performing MD near the boundaries for the accuracy of the interactions with the wall, and MC in the bulk because of the low computational costs. Using this method, the properties of the gas molecules confined between two hard walls of a nanochannel are studied. The effect of the size of the molecules on the simulation results is studied. As these properties near the wall of the nanochannel are shown to be dependent on the size of the gas molecules used in the simulations [20], we apply the hybrid method. The interactions near the solid walls are accurately simulated using MD simulations, and the bulk gas properties are studied using stochastic MC simulations. The hybrid MD-MC approach can also be used to simulate the interface between different phases as gas-solid, liquid-solid, liquid-gas.

In Sec. II, the physical model for a microchannel is presented, and a description of the MC, the MD, and our hybrid MD-MC simulation methods are given. We show that the MD, MC, and hybrid MD-MC simulations give similar results when hard-sphere interactions between particles are considered. We show that when changing the interaction model from hard-sphere to Lennard-Jones, the pure MD results differ considerably from the pure MC results. It is thus important to simulate accurately the interactions of the gas molecules near the wall and the interactions of the gas molecules with the wall. As MC simulations for the properties in the bulk can use different particle sizes, we also study how these results depend on the size of the gas molecules in the channel. In Sec. III, our method is validated using the hybrid MD-MC simulations results to study the density and temperature profiles in microchannels and nanochannels using different gas densities. Comparisons between pure MD, pure MC, and the hybrid MD-MC simulations are made. Last, comparisons with MD and MC computational costs are outlined.

II. THEORY

Here we give the theoretical background for the numerical and simulation results. First we specify our physical model for the microchannels, and then we describe the simulation methods used for our system, i.e., MC, MD, and our hybrid MD-MC simulation method. For the hybrid simulation method we describe the algorithm obtained by coupling MD and MC simulations having the same size of simulation particles.

A. The physical model

Our model to study the one-dimensional heat flow in a microchannel consists of two parallel infinite plates at a distance L apart from each other and of gas molecules confined between these two walls. An example is shown in Fig. 1. Both plates have their own temperature, T_1 and T_2, respectively, where this temperature is uniform on the plate surface and constant in time. The gas consists of spherical particles of diameter a and mass m, at temperature T. The density of the gas can be expressed as n, being the number of particles per unit of volume, or using a reduced density η, which also takes the particle sizes into account and is related to the number density as $\eta=\pi n a^3/6$ [3]. The mean free path of the gas particles is related to this reduced density. For a relatively dense gas with $\eta \approx 0.1$, the mean free path $\lambda\{\lambda = 1/[\sqrt{2}\pi a^2 n Y(\eta)]\}$ and the molecular diameter a have the

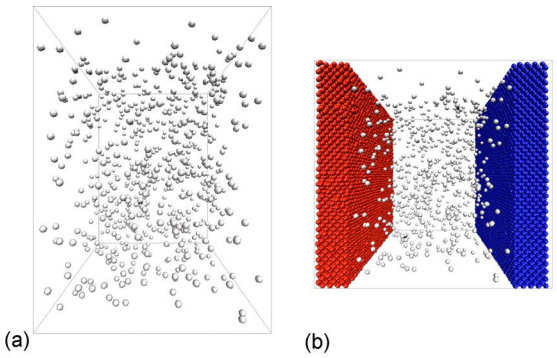

FIG. 1. (Color online) The model of a microchannel consists of a two parallel infinite plates at distance L apart from each other, and of gas molecules confined between these plates. Depending on the simulation method, the walls can be modeled (a) using boundary conditions or (b) explicitly.

same order of magnitude. The Y factor is the pair correlation function at contact; its dependence on η is introduced in the next section. The distance L between the plates, in the x direction, is always such that both plates are only a few mean free paths apart.

B. Monte Carlo methods

The first simulation method used is an extended version of the direct simulation Monte Carlo method. The method is based on the Enskog kinetic equation [9]. This Enskog equation is an extension of the Boltzmann equation to dense fluids and has the form

$$\frac{\partial F}{\partial t} + \xi \cdot \nabla F = J_E(F,F), \tag{1}$$

where $F(x,\xi,t)$ is the one-particle distribution function of the molecular velocity ξ. The collision integral $J_E(F,F)$ keeps the same binary structure of the corresponding Boltzmann term, but the colliding molecules occupy different positions in space and the collision frequency is modified by the factor Y which plays the role of an approximate pair correlation function [3,4]. In the standard Enskog theory (SET) [10] of the hard-sphere fluid, the representation of the pair distribution function is the product of two one-particle distribution functions times the pair correlation function $Y(n)$ in a state of uniform equilibrium evaluated at the contact point. In equilibrium, the relation between Y and the equation of state (EOS) is as given by Resibois and DeLeener [21]:

$$Y(n) = \frac{1}{nb}\left(\frac{p}{nkT} - 1\right), \tag{2}$$

p being the pressure and $b = 2\pi a^3/3$. The equation of state of the hard-sphere fluid cannot be given in a closed form, but various approximate expressions have been proposed. Carnahan and Starling [22] found a clever way to represent the hard-sphere gas EOS by a simple expression from which an approximate Y can be obtained. The approximation by Carnahan and Starling has been used here:

$$\frac{1 + \eta + \eta^2 - \eta^3}{(1-\eta)^3}, \tag{3}$$

where $\eta = \pi a^3 n/6$, yielding the Y function having the form

$$Y(\eta) = \frac{1}{2}\frac{2-\eta}{(1-\eta)^3}. \tag{4}$$

The expression for the mean free path given in the preceding section comes from the Enskog equation's collision term, which, in uniform distribution, takes the same form as the Boltzmann equation's collision term [23,24], except for the Y factor.

The important macroscopic quantities that we are computing in our MC simulations are the number density, the mean velocity, the temperature, the heat flux, and the stress. In terms of the one-particle distribution function F, these properties can be written as it follows: number density

$$n(x) = \int F(x,\xi) d\xi, \tag{5}$$

mean velocity

$$u(x) = \frac{1}{n(x)} \int \xi F(x,\xi) d\xi, \tag{6}$$

and temperature

$$T(x) = \frac{m}{3n(x)k} \int (\xi - u)^2 F(x,\xi) d\xi, \tag{7}$$

where k is the Boltzmann constant.

The heat flux vector (q) and the stress tensor (P) are both the sum of a kinetic and a potential part, i.e., $q = q_{kin} + q_{pot}$, and $P = P_{kin} + P_{pot}$. The kinetic heat flux and stress tensor are computed as

$$q_\alpha^{kin}(x,t) = \frac{m}{2} \int c_\alpha c^2 F(x,\xi,t) d\xi, \tag{8}$$

$$P_{\alpha\beta}^{kin}(x,t) = m \int c_\alpha c_\beta F(x,\xi,t) d\xi, \tag{9}$$

where $c = \xi - u$ is the peculiar velocity; α, β can be any of the x, y, or z directions; and $c^2 = \Sigma_{\beta=x,y,z} c_\beta{}^2$. The potential heat flux and stress tensor are computed as in [3,4]. In our simulations, where the two infinite plates are separated in the x direction, we are mainly interested in the x component of the total heat flux vector, q_x.

The Enskog equation can be solved numerically by means of a particle simulation method, as proposed by Frezzotti in 1997 [3,4], to study the one-dimensional steady heat flow in a dense hard-sphere gas. In this particle simulation method the molecules of the fluid are represented by mathematical particles, which we consider having the same size as the particles of the physical model (a). Each particle is characterized by its position $\vec{x}$ and its velocity $\vec{v}$. These particles are positioned in a simulation box [see Fig. 1(a)]. Because of the use of periodic boundary conditions in the directions parallel to plates, this box represents the infinite physical system described above. The plates are modeled using thermal wall

boundary conditions, implicating that particles that hit such a wall are reflected with a new velocity randomly chosen from a distribution corresponding to the temperature of that wall.

Due to their velocity the particles move through the flow-field region and can thus collide with each other. Important in this method is that the particle trajectories are not used to calculate collisions with other particles explicitly. Instead, the method uses a computationally much cheaper approach where collisions are performed stochastically. This calculation is obtained using the following scheme. Repeatedly, the particles are first advected and subsequently collisions are calculated stochastically. In the advection step, the particles are moved according to their velocities and the time-step size. During the collision step collision partners are selected from predescribed collision probabilities. This is done by dividing the system into cells. A particle in a given cell can collide with particles in nearby cells. The chance that two such particles really collide depends on their relative velocities and the binary collision integral $J_E(F,F)$. Whenever a collision is accepted the velocities are changed according to [3,4], ensuring the exact global conservation of momentum and energy.

Since the method is intrinsically designed to solve the unsteady Enskog equation, after preparing the particle system in a suitably chosen initial state, a number of time steps has to be computed until the transient dies out; then the sampling of the particle properties starts to be gathered and the time-averaged macroscopic quantities are obtained.

C. Molecular dynamics

The second simulation method to simulate the channels is molecular dynamics (MD). In an MD simulation the exact particle trajectories are calculated by computing all the forces that the particles exert upon each other. These forces are described by means of interaction potentials. A commonly used potential to describe the interactions between particles is the Lennard-Jones (LJ) potential

$$V_{LJ}(r) = \epsilon\left[\left(\frac{2R_{\mathrm{vdW}}}{r}\right)^{12} - 2\left(\frac{2R_{\mathrm{vdW}}}{r}\right)^{6}\right], \tag{10}$$

where ϵ is the interaction strength and R_{vdW} the van der Waals radius, a measure for the particle size. The LJ potential is mildly attractive as two molecules approach each other from a distance, but strongly repulsive when they come too close.

In order to simulate hard-sphere-like interactions using MD, truncated shifted Lennard-Jones (tsLJ) potentials were used for the interactions between gas molecules. This potential is defined as

$$V_{tsLJ} = \begin{cases} V_{LJ}(r) - V_{LJ}(r_c) & \text{if } r \leqslant r_c \\ 0 & \text{if } r > r_c, \end{cases} \tag{11}$$

where r_c is the cutoff radius. With a cutoff radius $r_c = 2R_{\mathrm{vdW}}$, this basically means that only the repelling part of the LJ potential is taken into account such that all the attractive interactions between particles situated at larger distances are ignored. The choice of ϵ determines how hard the particles are. This is demonstrated in Fig. 2 where the hard-sphere potential is compared with our potentials. For the tsLJ potential with $\epsilon = 1$ the particles are still relatively soft, i.e., the particles can partially overlap during a collision. When two particles come closer together than $2R_{vdW}$, they start to repel each other. When they come closer together, kinetic energy is converted to potential energy until all kinetic energy in the direction of the separation between the two particles has been converted. Then the two particles move away from each other where the potential energy is converted back to kinetic energy. A second measure for the particle size is thus given by the minimal distance between the two particles during such a collision, which we will refer to as the *collision diameter*. This collision diameter will be different for every collision, as the velocities of all particles are different, however on average this collision diameter will approximately equal that distance for which the pair interaction potential $V(r)$ equals one. As this minimum distance during a collision compares well to the size of the particles in the MC simulations we will use this collision diameter to fix the value for R_{vdW} in Eq. (7). Thus, for $\epsilon = 1$ the choice $2R_{\mathrm{vdW}} = 2^{1/6}a$ results in particles with average collision diameter a. For a stronger tsLJ potential with $\epsilon = 1000$ an average collision diameter a is obtained with the choice $2R_{\mathrm{vdW}} = 1.005a$. These particles are very close to hard spheres and thus barely overlap, such that the van der Waals radius is only slightly larger than $a/2$.

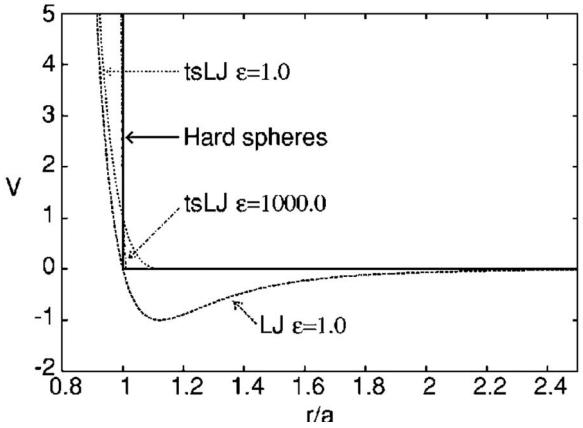

FIG. 2. Comparison of different potentials for the MD simulations. Shown are the Lennard-Jones (LJ) potential, the truncated shifted Lennard-Jones (tsLJ) potential for two different values of ε, and the hard-sphere potential.

Periodic boundary conditions are used again in the directions parallel to the plates. The plates can be modeled again using the same thermal wall boundary conditions as used for the MC simulations. However, with MD it is also possible to simulate the walls explicitly [see Fig. 1(b)]. Namely, an advantage of the MD method is that it is not only suited for simulating gases and liquids but also for crystals. With the MD method it is thus possible to model the walls and also the interaction of the gas particles with these walls explicitly. When the walls are simulated explicitly, LJ potentials are used to simulate the interaction of the particles in these walls. For the interactions of the molecules in the solid, the

standard LJ potential is used with $\epsilon=6$ in order to keep the crystal structure of the solid intact and to prevent the wall particles from evaporating and mixing with the gas molecules. The interactions between the wall particles and the gas particles and between gas particles mutually are modeled by weaker Lennard-Jones potentials or by a truncated shifted Lennard-Jones potential.

Thus, in MD both explicit wall and boundary conditions can be used to model the plates. The advantage of the use of boundary conditions is that much fewer particles are needed in the simulation and that the MC and MD methods can be compared more fairly on the same basis. The advantage of the use of explicit walls is that the interaction with the wall, which can be crucial for the total behavior, can be simulated much more accurately. Being able to include a more accurate desciption of the interface is a very important feature of the hybrid method.

Also from the MD simulations macroscopic properties can be derived, such as the density, the mean velocity, the temperature, the heat flux, and the stress. The heat flux vector q is given by the relation

$$\vec{q} = \frac{d}{dt}\sum_i \vec{r}_i E_i, \tag{12}$$

where $\vec{r}_i$ is the position, and E_i is the energy associated with particle i. This can be split again into a kinetic and a potential part

$$\vec{q}_{kin} = \sum_i E_i^{kin}\vec{v}_i = \frac{1}{2}\sum_i m_i v_i^2 \vec{v}_i, \tag{13}$$

$$\vec{q}_{pot} = \frac{1}{2}\sum_{i,j} (\vec{F}_{ij}\cdot\vec{v}_i)\vec{r}_{ij} + \sum_i E_i^{pot}\vec{v}_i, \tag{14}$$

where m_i and $\vec{v}_i$ are, respectively, the mass and the velocity of particle i, and $\vec{F}_{ij}$ and $\vec{r}_{ij}$ are the interaction force and separation vector between particles i and j. The stress vector is given by the relation

$$P_{\alpha\alpha} = \frac{1}{V}\sum_i m_i {v_\alpha}^2 - \frac{1}{V}\sum_{i,j} F_{ij\alpha} r_{ij\alpha}, \tag{15}$$

where α can be any of the x, y, or z directions, and V stands for the volume. The first term of the sum is the kinetic part of the stress vector, $P_{\alpha\alpha}^{kin}$, and the second term of the sum is the potential part of the stress vector, $P_{\alpha\alpha}^{pot}$.

D. The wall effects

Before describing the hybrid method, we compare results from pure MD and pure MC simulations. The reason for this is twofold: in the first place to check that MD and MC yield comparable results, and in the second place to see where the differences are.

First a comparison is made between MD and MC where thermal wall boundary conditions are used in both cases. The particles that are used are as described in the two previous sections, where for the MD, the tsLJ potential with $\epsilon=1$ is used. For the MC simulation 100 cells are used, having a width of 0.2λ. On average 200 particles are present per cell. The number of collisions is estimated per step from a stochastic process as described earlier, but to give an example, for $\eta=0.1$ the total number of collisions computed per step is around 5500, from which appoximately 470 are accepted as real collisions.

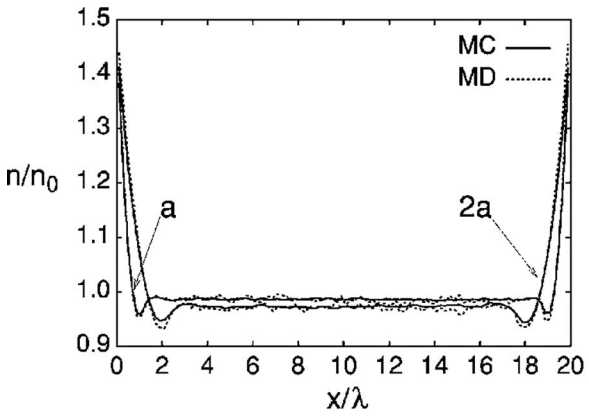

FIG. 3. Comparison between MD and MC density profiles n/n_0 for $\eta=0.1$, and $T_1=T_2=T=1.0$, for two different particle sizes: a and $2a$, and thermal wall boundary conditions. The MD particles are considered as having $\epsilon=1$.

First we characterize the influence of the particle size. The effect of the particle size on the simulation results is very small in the case of a dilute gas, but increases with η. In Fig. 3 the density profiles, both from MD and from MC, are shown for two systems with different particle sizes but with the same relatively high reduced density $\eta=0.1$. The reference number density n_0 is considered to be the flow-field number density at the initial flow temperature. The particles in the second system are twice as large as those in the first system. From this figure it is clear that for such high gas densities, the behavior is largely influenced by the particle size, especially near the walls. This is important, as in many DSMC simulations one particle usually represents several gas molecules instead of one single molecule. But these results show that for accurate simulations particles of the real physical size are needed, at least near the walls.

For a closer comparison between the MD and the MC density profile results we characterize the influence of different reduced densities on our simulation results for the gas in the microchannel. The effect of different gas densities, starting from a rarefied gas ($\eta=0.001$) to a dense gas ($\eta=0.25$), is shown in Fig. 4. These results show that for relatively dense gases ($\eta>0.05$), density oscillations occur near the walls of the microchannel. According to Frezzotti [3,4], the high density near the wall can be explained taking into account that when the distance of a molecule from the wall is less than the molecular diameter a, a portion of the molecule's surface is protected from collisions since there is no room for a collision partner. The molecule is therefore pushed against the wall, which explains the high density of the molecules near the hard wall. The oscillations in density near the wall at relatively dense gas up to the liquid density

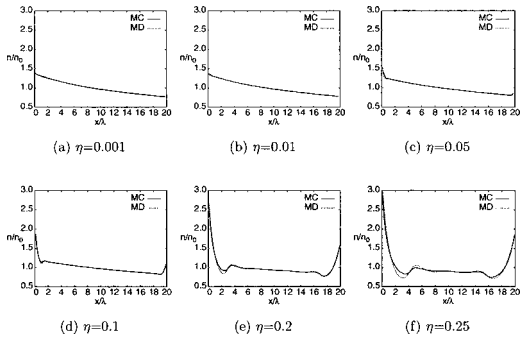

FIG. 4. Comparisons between MC and MD simulation results for different reduced densities (η's) and $T_1/T_2=1/2$, where MD particles having $\epsilon=1$, MC particles having size a, and thermal wall boundary conditions are considered.

is the effect of the particles packing near the hard wall [20].

Figure 4 also shows that the resulting MD and MC density profiles are comparable for all densities. For low densities the results are even identical, but for higher densities a larger and larger deviation is visible near the walls. Although the density profiles for both MC and MD have the same shape, small differences appear in the peak region as an effect of the different collision mechanisms. These differences increase in the peak regions near the wall as η increases. The temperature profiles for MD and MC simulations are also comparable.

When using the tsLJ potential with $\epsilon=1000$ for the particles in the MD simulations instead, the particles resemble hard spheres more closely. In Fig. 5, the resulting profiles of such an MD simulation for a reduced density $\eta=0.1$ are compared with the MC results. Here, not only the density and temperature profiles are compared but also the kinetic and potential heat flux and the kinetic and potential contribution to the stress. All profiles are in good agreement. Only near the boundaries the differences for the heat flux and the stress are visible. The MD results for the total stress have a small dip near the cold wall and a jump near the warm wall [Fig. 5(c)], and the total heat flux has a jump near the cold wall and a sink near the warm wall [Fig. 5(d)], whereas the total stress and heat flux should be constant. The deviations

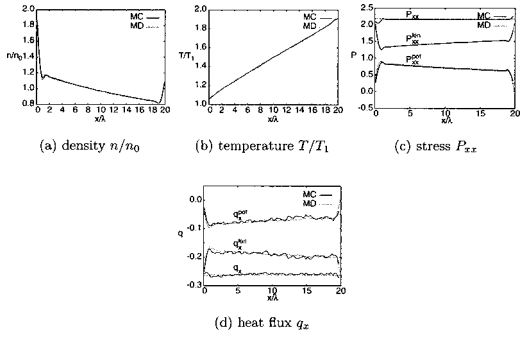

FIG. 5. Comparison between results from pure MD and pure MC, for $\eta=0.1$ and $T_1/T_2=1/2$, where MD particles having a larger ϵ to model hard spheres are used ($\epsilon=1000$), MC particles having size a, and thermal wall boundary conditions are considered. P and q are normalized to n_0kT_1 and $m^{-1/2}n_0(kT)^{3/2}$, respectively.

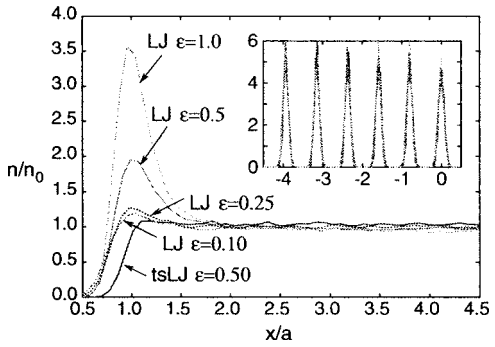

FIG. 6. Comparison between MD simulations near the wall for the relative number density n/n_0, when using different gas-wall interaction strengths in the LJ potential ($\epsilon=0.10,0.25,0.50,1.0$), and $\epsilon=0.50$ in the truncated shifted LJ potential, when $\eta=0.0261$. In the inset the different layers of the crystal structure of the wall can be discerned, the first layer being situated at $x=0$.

near the walls in MD are caused because the interaction with the walls is not taken into account when calculating the stress and heat flux.

Next, we study the effect of explicitly simulating the wall instead of using thermal wall boundary conditions in MD. When explicitly including the walls within MD by modeling the interactions between the hard-sphere gas molecules using a truncated shifted Lennard-Jones potential, and between the wall-gas and the wall-wall molecules using a Lennard-Jones potential, we see that the results of pure MD simulations start to differ considerably when different strengths for the wall-gas interactions are used. This can be seen in Fig. 6. The comparisons between the MD simulations for a dilute gas ($n_0=0.05$, $\eta=0.0261$), using different interaction strengths (ϵ's) for the wall-gas interactions, show that high-density peaks appear in MD even in the case of a dilute gas. The molecules near the wall are attracted by the wall, and the height of these peaks is increasing with ϵ. When increasing the interaction strength ϵ, it is energetically more favorable for a molecule to have many neighbors, as more neighboring molecules means more energetic contributions. As the gas is dilute, this explains the preference of particles to be near the wall molecules. The hard-sphere model using a truncated shifted Lennard-Jones, potential is not able to predict these density peaks near the wall for low gas densities. In Fig. 6 we can see that the position of these peaks is situated at one molecular diameter from the wall. The position of the first layer of molecules in the wall is situated at $x=0$, as can be seen in the inset in Fig. 6, where the density profile for the layers of molecules in the solid wall is shown.

These results show that the accuracy of the simulation results depends on how accurately we model the interactions between the gas molecules and between the gas and wall molecules, and we conclude that pure MC is not adequate to describe microchannels and nanochannels accurately enough for the boundary properties. On the other hand, MD simulations can be very accurate, but to model a complete microchannel, MD simulations are too slow.

E. Hybrid molecular dynamics–Monte Carlo methods

In order to perform more efficient simulations, we propose a simulation method that combines the advantages of

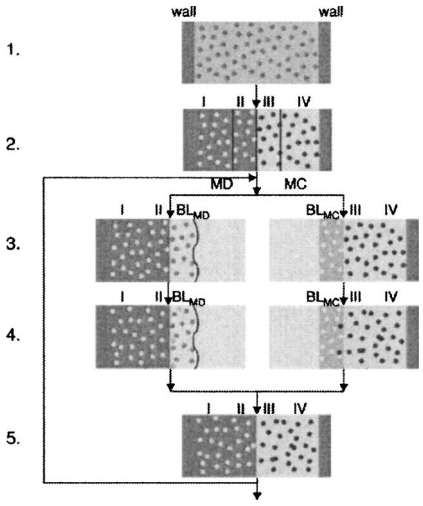

FIG. 7. The coupling of the MD and MC simulations is obtained via an interface layer. The curved-line boundary of the MD boundary layer BL_{MD} corresponds to the soft (movable) border.

the molecular dynamics (MD) and Monte Carlo (MC) simulations. How this is done is shown schematically in Fig. 7 for the case where MD is used in the left half of the simulation domain (regions I and II) and MC in the right half (regions III and IV).

Our simulation algorithm consists of the following steps.

(1) First an initial configuration for the whole system is created. The positions of the particles are randomly generated in the simulation domain, and the velocities of the particles are generated from a Maxwell-Boltzmann distribution.

(2) The particles in the region in which MD is performed are sent to the MD simulator and analogously the particles in the MC range are sent to the MC simulator.

(3) However, the MD simulation needs information from the neighboring MC particles and vice versa. This is obtained by creating an interface coupling the two subdomains. The MD simulation is extended with a buffer layer (BL_{MD}) to which the information of the MC particles in region III are copied, and analogously the MC simulation is extended with a buffer layer (BL_{MC}) to which the information of the MD particles in region II are copied.

(4) Now both the MD and the MC simulator can run in parallel. This implies that the MC simulator performs one iteration, updating the positions and velocities of all its particles. Parallel to this, the MD simulator should simulate the same time interval. Because the time-step size that can be made in one MD iteration is usually small compared to the time-step size in MC, we have to do a number of MD time steps for every single MC simulation step.

(5) The information for the whole system is now obtained by recombining regions I and II from MD with regions III and IV from MC. And the simulation can be continued with a new iteration of the hybrid procedure by restarting from step 3.

In the following we will elaborate more on the most important aspects of the method. The first important point is about updating the buffer layers after each iteration of the hybrid method. A straightforward approach is to provide the buffer layers BL_{MD} and BL_{MC} with a new copy of regions III and II, respectively. We have previously investigated [25] the coupling between the two methods in this way which was realized by importing and exporting particles from one simulator to the other. However, as we couple two simulation methods based on a different mechanism of computing the interactions between particles, problems are encountered as expected when trying to couple the less detailed method with the more accurate method. This is the case for coupling the MC and MD particle domains. Whereas for MD-to-MC particle coupling, particles from the MD domain can be imported directly into the MC domain using the exact positions and velocities, this cannot be done for MC-to-MD particle coupling, as in MC simulations particles can overlap each other. Imported into the MD domain, this would result in very large forces, leading to a high temperature jump in the interface layer caused by energy conservation problems. An option is to reposition the overlapping particles. A new random position is chosen which is accepted or rejected according to a probability distribution depending on the potential energy of the particle at that new position. However, because this has to be done every iteration, an equilibrium MD configuration is never formed.

Here an alternative method is used for the MC-to-MD coupling, where macroscopic properties are copied instead of single particles. In this method the positions and velocities of the particles in the MD buffer layer (BL_{MD}) are kept and subsequently scaled to match the macroscopic quantities from MC region III. To allow also gradients in these quantities, the MD buffer layer (BL_{MD}) and MC layer III are divided into subcells, and the average properties of the particles in the subcells are imported from the MC domain. To set the temperature and momentum in the buffer layer, the particle velocities in the buffer layer are rescaled per subcell according to the corresponding imported MC average temperature and momentum per subcell from region III.

Because the positions of the particles are kept, a wall has to be added at the end of the MD buffer layer to prevent the particles from leaving this region. Considering this border as a hard wall can influence significantly the simulation results in this region and can affect also simulation results in region II. To prevent the additional wall from influencing the simulation results, a hard wall has not been used, but instead a harmonic potential that pushes the particles back into the buffer region: a soft border.

Updating the density in the buffer layer is not done per subcell because of the problems encountered with energy conservation when generating or removing particles in the MD subdomain. Instead of removing and adding particles, we adapt the density in a way analogous to Berendsen pressure scaling [26]. This is done by moving the soft border that limits the MD buffer layer. This border is shifted to the right if the density has to be decreased and to the left if the density has to be increased. For instance, if the density in the buffer layer is higher than the density in region III, the border can be moved to the right such that the volume of the buffer layer is increased while keeping the same number of particles. This border can move to the right or to the left with a maximum of $\lambda/2$. Only if the density has to be changed more are particles added or removed. This will only happen when the

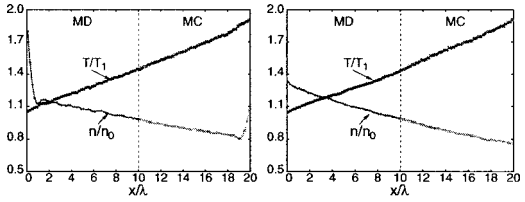

FIG. 8. The density and temperature profiles in the channel as obtained from the hybrid MD-MC simulations for two different densities when $T_2/T_1=2$ and $L=20\lambda$. The domain is split into two subdomains, the left one being MD (50%), and the right one MC (50%). MD particles having $\epsilon=1$ and thermal wall boundary conditions are considered.

system is still far from equilibrium. Once the system reaches the equilibrium state, the flux of particles from one domain to another will become constant and the process of updating the density in the buffer layer BL_{MD} reduces to shifting the border.

Our hybrid simulator is constructed as follows: It consists of three components, the MD component for the MD simulations, the MC component for the MC simulations, and an interface component between the first two components, coupling the MD and MC simulations. The MD and MC components are independent; the MD and MC steps were computed by two different independent codes based on already developed software [27] which was implemented in different programming environments, the MC simulator in FORTRAN77, and the MD simulator in C. Being independent, the MD and MC components can reside on different computers, and can run in parallel being synchronized and coupled by an interface written in PYTHON.

III. RESULTS AND DISCUSSION

In this section we validate our hybrid MD-MC simulation results by comparing them with the pure MC and pure MD simulation results. We consider two situations for the hybrid method, when the domain is equally split into the MD and MC subdomains, and when the domain is split into three subdomains, two MD subdomains near the walls, and one MC in the middle. We show that our method is able to implement very accurately the interface between the different domains, and the results are similar to pure MD simulation results. We continue by comparing the timings for the MD, MC, and hybrid MD-MC methods, and also the accuracy of the simulation results using MC, MD, and hybrid MD-MC methods. In all these simulations thermal wall boundary conditions are considered both in MC and in MD, and MD particles are considered as having $\epsilon=1$.

A. Comparison between MD, MC, and hybrid MD-MC results

To begin, we split the domain equally into two subdomains, one half being the MD subdomain, and the other half the MC subdomain, as in Fig. 7. The temperature of the warm wall T_2 is twice the temperature of the cold wall T_1. Figure 8 shows the hybrid MD-MC simulation results for the density and temperature profile in the channel when $L=20\lambda$ and $T_2/T_1=2$, both for a dense gas ($\eta=0.1$) and for a more dilute gas ($\eta=0.01$). Our simulation profiles are equal to pure MD and pure MC simulation results, proving that we can use the hybrid method to couple MD and MC simulations.

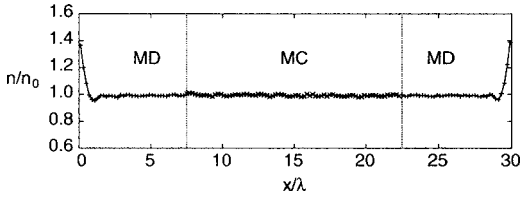

FIG. 9. The density profile in the channel for $\eta=0.1$, $T_2/T_1=1$, and $L=30\lambda$ as obtained from a hybrid MD-MC simulation when the domain is split into three parts: two MD domains (25%) near the walls and one MC domain (50%) in the middle. MD particles having $\epsilon=1$ and thermal wall boundary conditions are considered.

The next step is then to use MD near both channel walls and MC in the middle for the bulk. In our implementation this means adding one extra MD component, which can again run in parallel with the other two. Figure 9 shows the density profile in the channel for such a simulation, for the case when both walls and the gas are at the same temperature $T_1=T_2=T$.

B. Comparison of simulation times for the MD, MC, and hybrid MD-MC methods

We have computed the simulation times for the system consisting of 20 000 particles. Comparisons between pure MD, pure MC, and hybrid MD-MC simulation times were performed for simulations consisting of 500 combined MD-MC iterations, and for different reduced densities ($\eta=0.1$, $\eta=0.01$). For a dense gas ($\eta=0.1$), the 500 combined iterations consisted of 500 MC steps and 2500 MD steps, while for a dilute gas ($\eta=0.01$) these iterations consisted of 500 MC steps and 30 000 MD steps, because 60 MD steps are needed for every MC iteration. For the coupled MD-MC simulations, two situations were considered. In the first case the simulation domain is equally divided between MD and MC. In the second case the MD domain covers only 10% of the whole domain and 90% is the MC domain. The timing results are presented in Table I. We notice that the speedup

TABLE I. Simulation times for 500 combined iterations and 20 000 particles.[a]

Timings	$\eta=0.1$	$\eta=0.01$
Pure MC	2.4	2.3
Pure MD	203.3	1169.6
MD (50%) - MC (50%)	246.5	1162.9
MD (10%) - MC (90%)	43.4	206.9

[a]For $\eta=0.1$, simulation times are computed for 500 MC steps and 2500 MD steps. For ($\eta=0.01$), timings are done for 500 MC steps and 30 000 MD steps.

when using the hybrid MD-MC method for 50% MD and 50% MC is very small when compared to pure MD simulation times, but this speedup increases drastically when the bulk is larger than the region near the wall. For example, when the MC domain is extended to 90% of the simulation domain and the MD domain is reduced to 10% of the simulation domain, the speedup of the simulations increases roughly with a factor of 5. We notice also that this efficiency is independent of density.

C. Comparison between accuracy of MD, MC, and hybrid MD-MC results

We measure the accuracy of the simulation results for the number density n, when $\eta=0.1$, by computing the deviations of the simulation results using the method mx from the pure MD simulation results that are considered to be the exact solution. The deviations are given by the relation $\sqrt{(n_{mx}-n_{MD})^2}/n_{MD}$, where n_{mx} stands for the density results when using the simulation method mx. The mx simulation method could be the MC, MD, or hybrid MD-MC with different sizes of the MD and MC domains. The deviations of the MC simulation results are found to be around 0.9%. When the hybrid method is used, we noticed that the deviations decrease with a factor from two to three, and are between 0.32%–0.42%. This shows that using the hybrid MD-MC simulation method we get more accurate results compared to the pure MC simulation results and faster simulations compared to the pure MD simulation times.

An important remark is that the size of the buffer layer of the MD domain BL_{MD} influences the accuracy of the results. The larger the size of this buffer layer, the smaller the influence of the soft boundary wall and the more accurate the results. Hybrid simulation for systems having different sizes of the buffer layer BL_{MD} and number of subcells in this buffer layer have been compared with pure MD simulations, resulting in the choice for a width of 3λ for BL_{MD} and 10 subcells.

IV. CONCLUSION

By coupling different simulation methods we can combine in one hybrid method the advantages of these simulation methods. We have coupled two particle simulation methods, namely molecular dynamics (MD) and Monte Carlo (MC). With the hybrid MD-MC approach we are able to study the density, temperature, heat flux, and stress profiles for dilute and dense gases in microchannels and nanochannels. This method couples the MD simulations near the boundary for the accuracy of the interaction with the wall and MC in the bulk because of low computational costs. Comparisons between the MC and MD simulation results, with MD and MC particles having the same size, are in good agreement, but they differ near the boundaries for high densities. When these particles are not simulated as hard spheres but using the Lennard-Jones potential, the behavior near the wall is strongly influenced by the strength of the interactions such that peaks appear in MD simulations even in the case of a dilute gas. We studied the accuracy of our hybrid simulation results and compared them with the exact MD and also with the MC simulation results. Comparisons between pure MD, pure MC, and hybrid MD-MC simulations show that our hybrid simulation profiles are correct, both for a dilute and a dense gas. Comparisons between simulation times using pure MC, pure MD, and hybrid MC-MD methods have been given. The results show that the speedup when using 50% of the domain for MD simulations and 50% for MC simulations is very small compared to pure MD simulation times, but this speedup increases drastically for more realistic situations where the region near the wall is small compared to the bulk region. The hybrid MD-MC simulation results are also very accurate compared to the pure MC simulation results and the hybrid simulations are faster compared to the pure MD simulation times.

ACKNOWLEDGMENTS

The authors thank Professor A. Frezzotti and Professor A. L. Garcia for their stimulating discussion of and insights into the MC simulation techniques for the one-dimensional heat flow.

[1] R. R. Schmidt and B. D. Notohardjono, IBM J. Res. Dev. **46**, 739 (2002).
[2] G. A. Bird, *Molecular Gas Dynamics and the Direct Simulations of Gas Flows* (Clarendon Press, Oxford, 1994).
[3] A. Frezzotti, Eur. J. Mech. B/Fluids **18**, 103 (1999).
[4] A. Frezzotti, Phys. Fluids **9**, 1329 (1997).
[5] D. Frenkel and B. Smit, *Understanding Molecular Simulation* (Academic, San Diego, 1996).
[6] F. J. Alexander, A. L. Garcia, and B. J. Alder, Phys. Rev. Lett. **74**, 5212 (1995).
[7] F. J. Alexander, A. L. Garcia, and B. J. Alder, Physica A **240**, 196 (1997).
[8] A. L. Garcia, *Numerical Methods for Physics* (Prentice Hall, Englewood Cliffs, NJ, 1994) Chap. 1.
[9] D. Enskog, K. Sven. Vetenskapsakad. Handl. **63**, 3 (1922).
[10] H. van Beijeren and M. H. Ernst, Physica (Amsterdam) **68**, 437 (1973).
[11] J. M. Montanero and A. Santos, Phys. Fluids **9**, 2057 (1997).
[12] J. M. Montanero and A. Santos, Phys. Rev. E **54**, 438 (1996).
[13] K. Nanbu, *Proceedings of the 15th International Symposium on Rarefied Gas Dynamics*, edited by V. Boffi and C. Cercignani (Teubner, Stuttgart, 1986).
[14] H. S. Wijesinghe, R. D. Hornung, A. L. Garcia, and N. G. Hadjiconstantinou, J. Fluids Eng. **126**, 768 (2004).
[15] H. S. Wijesinghe, A. L. Garcia, and N. G. Hadjiconstantinou, Int. J. Multiscale Comp. Eng. **3**, 189 (2004).
[16] R. Delgado-Buscalioni and P. V. Coveney, J. Chem. Phys. **119**, 978 (2003).

[17] R. Delgado-Buscalioni and P. V. Coveney, Phys. Rev. E **67**, 046704 (2003).

[18] N. G. Hadjiconstantinou and A. T. Patera, Int. J. Mod. Phys. C **8**, 967 (1997).

[19] A. Kucaba-Pietal and Z. P. Zbigniew Walenta, Turbulence **10**, 77 (2004).

[20] S. V. Nedea, A. J. H. Frijns, A. A. van Steenhoven, and A. P. J. Jansen, *ASME Second International Conference on Microchannels and Minichannels*, edited by S. G. Kandlikar (ASME, Rochester, NY, 2004), pp. 289–296.

[21] P. Resibois and M. DeLeener, *Classical Kinetic Theory of Fluids* (Wiley, New York, 1977).

[22] N. F. Carnahan and K. E. Starling, J. Chem. Phys. **51**, 635 (1969).

[23] C. Cercignani, *Mathematical methods in kinetic theory* (Plenum, New York, 1990).

[24] S. Chapman and T. G. Cowling, *The mathematical theory of nonuniform gases* (Cambridge University Press, Cambridge, U.K., 1960).

[25] A. J. H. Frijns, S. V. Nedea, A. J. Markvoort, A. A. van Steenhoven, and P. A. J. Hilbers, in *Workshop on Modelling and Simulation of Multi-Scale Systems, ICCS 2004*, Pt. IV, edited by Marian Bubak, G. Dick van Albada, Peter M. A. Sloot, Jack J. Dongarra (Springer-Verlag, Berlin, 2004), pp. 666–671.

[26] H. J. C. Berendsen, J. P. M. Postma, W. F. van Gunsteren, A. DiNola, and J. R. Haak, J. Chem. Phys. **81**, 3684 (1984).

[27] K. Esselink and P. A. J. Hilbers, J. Comput. Phys. **106**, 108 (1993).